This is a post-peer-review, pre-copyedit version of an article published in IEEE Antennas and Wireless Propagation Letters.
The final authenticated version is available online at: http://dx.doi.org/10.1109/LAWP.2017.2689803

Objective Relaxation Algorithm for Reliable Simulation-Driven Size Reduction of Antenna Structures

Slawomir Koziel, *Senior Member, IEEE*

***Abstract*—This letter investigates reliable size reduction of antennas through electromagnetic-driven optimization. It is demonstrated that conventional formulation of the design task by direct footprint miniaturization with imposing constraints on electrical performance parameters may not lead to optimum results. The reason is that—in a typical antenna structure—only a few geometry parameters explicitly determine the antenna footprint, and therefore sensitivity of antenna size to other parameters is zero. At the same time, finding the genuine optimum requires adjustment of all parameters as the optimum is determined by the tradeoff between the size and other figures of merit such as reflection characteristic. Here, an alternative design methodology is proposed that involves relaxation between size reduction and matching improvement. Our methodology is demonstrated using two examples of ultrawideband antenna structures. It is superior over the conventional approach in terms of the optimized antenna size achieved. Experimental validation of the results is also provided.**

***Index Terms*—Antenna design, miniaturization, relaxation algorithm, simulation-driven design, surrogate modeling.**

I. Introduction

CONTEMPORARY antenna design is a complex process where several objectives have to be taken into account [1]. Among them, reduction of the physical size of the structure becomes more and more important in many applications such as handheld and wearable devices [2] or internet of things [3]. Unfortunately, making the antenna structure more compact leads to degradation of electrical performance parameters, primarily reflection response, but also radiation figures, efficiency, etc. Representative examples are ultrawideband (UWB) antennas where diminishing the footprint is associated with poor matching at the lower frequencies due to shortening of the current path [4]. This difficulty can be alleviated by means of various topological modifications of the antenna geometry such as I-shaped [5] or L-shaped stubs [6], protruded ground plane structures [7], matching transformers [8], slits below the feedline [6], or uniplanar monopole designs [9].

Manuscript received February 24, 2017; accepted March 28, 2017. Date of publication March 31, 2017; date of current version July 17, 2017. This work was supported in part by the Icelandic Centre for Research under Grant 163299052, and in part by the National Science Centre of Poland under Grant 2014/15/B/ST7/04683.

The author is with the School of Science and Engineering, Reykjavik University, Reykjavík 101, Iceland, and also with the Faculty of Electronics, Telecommunications and Informatics, Gdansk University of Technology, Gdańsk 80-233, Poland (e-mail: koziel@ru.is).

Color versions of one or more of the figures in this letter are available online at http://ieeexplore.ieee.org.
Digital Object Identifier 10.1109/LAWP.2017.2689803

The techniques mentioned above increase geometrical complexity of the antenna and introduce additional parameters that have to be adjusted to satisfy given performance requirements. Ideally, all antenna parameters should be tuned simultaneously: Due to complex interrelations between antenna dimensions and antenna characteristics, simple means such as parameters sweeping are very laborious and fail to identify optimum dimensions. Automated adjustment of all relevant parameters can be realized using numerical optimization techniques. For size reduction, constrained optimization is a necessity because the required level of electrical performance parameters, in particular, antenna matching, has to be maintained. A practical way of implementing such a process is to consider the antenna footprint as a primary objective while handling the reflection response using a penalty function approach [10], [11].

Despite conceptual simplicity, the approach of [11] exhibits a fundamental shortcoming: In many practical problems and depending on structure parameterization, the antenna size explicitly depends on only some of the geometry parameters (e.g., substrate dimensions, etc.) but does not depend on others (e.g., radiator size and shape, etc.), which leaves only a few degrees of freedom when optimizing for minimum footprint. Even though other parameters are involved indirectly through a penalty function handling reflection response, the optimization problem becomes very challenging: The constrained objective function may become multimodal and, consequently, difficult to handle using local optimization routines [12], [13] (otherwise preferred due to lower computational complexity over, e.g., evolutionary algorithms [14]).

In this letter, an alternative formulation of the design problem is proposed along with the optimization algorithm where minimization with respect to the antenna size and the maximum in-band reflection are interleaved in the course of the optimization run. Switching between size- and matching-oriented objective functions is realized upon accomplishing successful iteration of the trust-region-based gradient search and allows for utilization of all antenna parameters. Both the conventional and the proposed approach are executed over the same parameter space. As demonstrated, the proposed approach leads to better results, both in terms of the final antenna footprint and the quality of the antenna response. Numerical results are validated experimentally.

II. Size Reduction by EM-Driven Optimization

In this section, we formulate explicit size reduction problem and briefly outline the conventional methodology with a penalty function approach utilized to control the antenna reflection response [10]. We also introduce the proposed relaxation algorithm alleviating the issue of limited number of geometry parameters directly affecting the antenna size.

A. Formulation of Size-Reduction-Oriented Design Problem

The full-wave electromagnetic (EM)-simulated model of the antenna of interest will be denoted as $\boldsymbol{R}(\boldsymbol{x})$. Here, $\boldsymbol{x}$ represents independent designable parameters of the structure that are to be adjusted in the optimization process. We are interested in two figures of merit: antenna size denoted by $\boldsymbol{A}(\boldsymbol{x})$, and its reflection characteristic, specifically the maximum in-band reflection denoted as $S(\boldsymbol{x})$. For UWB antennas, we have $S(\boldsymbol{x}) = \max\{|S_{11}(\boldsymbol{x})|_{3.1\,\text{GHz to }10.6\,\text{GHz}}\}$.

Explicit reduction of the antenna size, which is the primary goal, requires that one attempt to minimize $A(\boldsymbol{x})$ while maintaining acceptable electrical performance parameters, here represented by a reflection level, for example, $|S_{11}| \leq -10$ dB in the entire UWB range. In order to handle both A and S, the following formulation of the problem was suggested in [10]:

$$\boldsymbol{x}^* = \arg\min_{\boldsymbol{x}} U_A(\boldsymbol{R}(\boldsymbol{x})) = \arg\min_{\boldsymbol{x}} U_A(A(\boldsymbol{x}), S(\boldsymbol{x})). \quad (1)$$

In (1), U_A is an objective function that encodes the design specifications, whereas $\boldsymbol{x}^*$ is the optimum design to be found. In [10], U_A was defined as

$$U_A(A(\boldsymbol{x}), S(\boldsymbol{x})) = A(\boldsymbol{x}) + \beta \cdot c(S(\boldsymbol{x}))^2. \quad (2)$$

Formulation (2) permits minimization of the antenna size A and to enforce S to satisfy the -10-dB threshold. Here, β is a penalty factor (we use $\beta = 1000$ in our numerical experiments), whereas c is a penalty function defined as $c(S(\boldsymbol{x})) = \max S(\boldsymbol{x}) + 10)/10,\ 0\}$. It should be emphasized that c only contributes to (2) if the reflection requirement is violated. Also, (2) can be easily generalized to handle multiple performance requirements by defining $U_A(A(\boldsymbol{x}), \ldots) = A(\boldsymbol{x}) + \beta_1 \cdot c_1(\boldsymbol{x})^2 + \ldots + \beta_p \cdot c_p(\boldsymbol{x})^2$, where p is the total number of requirements concerning, e.g., reflection, efficiency, gain, etc.

B. Optimization Algorithm

Problems (1) and (2) can be solved using any available numerical optimization algorithm (e.g., direct or surrogate-based optimization (SBO) approach [15]). Here, a trust-region-embedded gradient search algorithm is utilized that finds a sequence $\boldsymbol{x}^{(i)}$, $i = 0, 1, \ldots$, of approximations to $\boldsymbol{x}^*$ as

$$\boldsymbol{x}^{(i+1)} = \arg \min_{\boldsymbol{x};\ ||\boldsymbol{x}-\boldsymbol{x}^{(i)}|| \leq \delta^{(i)}} U_A(\boldsymbol{L}^{(i)}(\boldsymbol{x})). \quad (3)$$

The model $\boldsymbol{L}^{(i)}$ is a linear expansion of $\boldsymbol{R}$ at $\boldsymbol{x}^{(i)}$ defined as

$$\boldsymbol{L}^{(i)}(\boldsymbol{x}) = \boldsymbol{R}\left(\boldsymbol{x}^{(i)}\right) + \boldsymbol{J_R}\left(\boldsymbol{x}^{(i)}\right) \cdot \left(\boldsymbol{x} - \boldsymbol{x}^{(i)}\right) \quad (4)$$

where the Jacobian $\boldsymbol{J}_R$ is estimated using finite differentiation. The trust region radius $\delta^{(i)}$ is adjusted using the standard rules [16] based on the gain ratio $\rho = [U_A(\boldsymbol{R}(\boldsymbol{x}^{(i+1)}) - U_A(\boldsymbol{R}(\boldsymbol{x}^{(i)})]/[U_A(\boldsymbol{L}^{(i)}(\boldsymbol{x}^{(i+1)}) - U_A(\boldsymbol{L}^{(i)}(\boldsymbol{x}^{(i)})]$: increased if $\rho > \rho_{\text{incr}}$ (typically, $\rho_{\text{incr}} = 0.75$), decreased if $\rho < \rho_{\text{decr}}$ (typically, $\rho_{\text{decr}} = 0.25$). The new iteration point $\boldsymbol{x}^{(i+1)}\boldsymbol{x}$is only accepted if $\rho > 0$. Furthermore, because—by definition—we have that $\boldsymbol{J}_L(\boldsymbol{x}^{(i)}) = \boldsymbol{J}_R(\boldsymbol{x}^{(i)})$, objective function improvement is guaranteed for sufficiently small values of δ. Note that reduction of $U(\boldsymbol{R}(\boldsymbol{x}))$ leads to reducing the antenna footprint [cf., (2)].

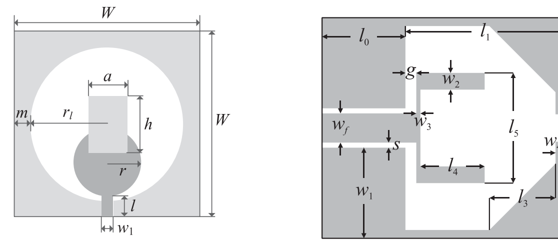

(a) (b)

Fig. 1. Geometries of UWB antennas considered for demonstrating the objective relaxation algorithm: (a) antenna I [17] and (b) antenna II [18].

C. Improved Formulation: Objective Relaxation

Formulation (2), although simple and straightforward, does not take into account the fact that in a typical antenna structure, the footprint explicitly depends on only a few geometry parameters [e.g., on two out of six parameters in the structure of Fig. 1(a)]. At the same time, electrical performance usually depends on all parameters. As a consequence, minimization of U_A becomes a difficult problem and may lead to a local optimum (note that gradient of the primary objective $A(\boldsymbol{x})$ is zero for all variables that do not directly determine the antenna footprint!). The primary issue is that formulation (2) introduces high nonlinearity of the functional landscape to be handled in the course of the optimization process along the boundary of the feasible region (i.e., where $S(\boldsymbol{x}) \approx -10$).

As a mean to alleviate this difficulty, in this letter, we propose a different approach, where minimization of the objective U_A is interleaved with minimization of the maximum reflection, i.e., the objective function

$$U_S\left(\boldsymbol{R}(\boldsymbol{x})\right) = U_S\left(S(\boldsymbol{x})\right) = S(\boldsymbol{x}). \quad (5)$$

The algorithm works as follows:

1) Find $\boldsymbol{x}^{(0)} = \text{argmin}\{\boldsymbol{x} : S(\boldsymbol{x})\}$;
2) Set $i = 0$;
3) Solve one iteration of (3) to find $\boldsymbol{x}^{(i+1)}$;
4) Solve

$$\boldsymbol{x}^{(i+2)} = \arg \min_{\boldsymbol{x};\ ||\boldsymbol{x}-\boldsymbol{x}^{(i+1)}|| \leq \delta_S^{(i)},\ A(\boldsymbol{x}) \leq A(\boldsymbol{x}^{(i+1)})} U_S(\boldsymbol{L}^{(i+1)}(\boldsymbol{x})). \quad (6)$$

5) Set $i = i + 2$;
6) If termination condition is not satisfied, go to 3, else END.

The optimization process begins in Step 1 by optimizing the antenna for best matching, which provides a feasible (from the point of view of the requirement $S(\boldsymbol{x}^{(0)}) \leq -10$) starting point for subsequent miniaturization. Steps 3 and 4 in the above-mentioned algorithm are executed until the iteration is successful, i.e., the gain ratio {e.g., $[U_A(\boldsymbol{R}(\boldsymbol{x}^{(i+1)}) - U_A(\boldsymbol{R}(\boldsymbol{x}^{(i)})]/[U_A(\boldsymbol{L}^{(i)}(\boldsymbol{x}^{(i+1)}) - U_A(\boldsymbol{L}^{(i)}(\boldsymbol{x}^{(i)})]$ in case of (3)} is positive. The trust region radii δ and δ_S are independent for (3) and (6) because the functional landscapes of U_A and

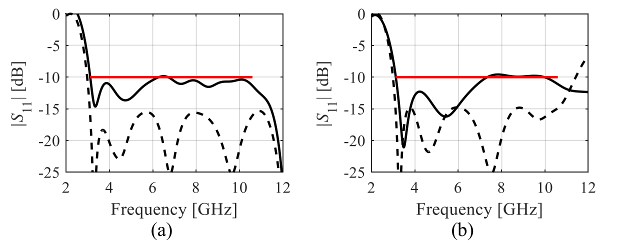

Fig. 2. Reflection responses of antennas I and II, optimization for best matching (- - -), optimization for size using relaxation (—): (a) antenna I and (b) antenna II.

U_S are generally different and the steps taken by the respective optimizers may be different. Interleaving reduction of the antenna footprint with matching improvement allows us to push the current iteration point back to the interior of the feasible region (from the point of view of the condition $S(\boldsymbol{x}) \leq -10$), which facilitates further size reduction after switching back to the objective function (2). When using only (2), the optimization algorithm may have difficulties in exploring the boundary of the feasible region. It should also be reiterated that both the original and the proposed method operate in the same design space.

III. Design Case Studies

Here, we demonstrate the proposed objective relaxation algorithm using two examples of planar UWB antennas. We also provide comparison to the conventional approach as well as experimental verification of the optimized designs.

A. Antenna Structures

Both considered antennas are implemented on Taconic RF-35 substrate ($h = 0.76$ mm, $\varepsilon_r = 3.5$). The first structure, a circular slot antenna with a rectangular patch (antenna I [17]) is shown in Fig. 2(a). The design variables are $\boldsymbol{x}_{\rm I} = [a\, l\, h\, r_l\, r\, m]^T$. Here, variables a and h are relative with respect to r_l, $W = 2r_l + 2m$ is dependent, whereas $w_1 = 2.8$ mm is fixed to ensure 50-Ω line impedance. The computational model of the structure is implemented in CST (∼870 000 mesh cells, simulation time 3 min). The second antenna {antenna II [18], Fig. 1(b)} is a uniplanar structure composed of a driven element in the form of fork-shaped radiator fed through a coplanar waveguide and an open slot. The design variables are: $\boldsymbol{x}_{\rm II} = [l_0\, l_1\, l_{2r}\, l_{3r}\, l_4\, l_5\, w_1\, w_2\, w_3\, w_4\, g]^T$. Parameters $w_f = 3.5$ and $s = 0.16$ to ensure 50 Ω input impedance, whereas variables $l_2 = (0.5w_f + s + w_1) \cdot \max l_{2r}, l_{3r}$ and $l_3 = (0.5w_f + s + w_1) \cdot l_{3r}$. The EM model of the antenna is also implemented in CST (∼400 000 mesh cells, simulation time 2 min).

B. Numerical Results and Benchmarking

Antennas I and II have been optimized for minimum size using the reference approach of Sections II-A and II-B, then using the proposed methodology of Section II-C. The termination condition for the optimization process is $||\boldsymbol{x}^{(i+1)} - \boldsymbol{x}^{(i)}|| < \varepsilon_1$ OR $\delta^{(i)} < \varepsilon_2$ OR $\delta_S^{(i)} < \varepsilon_3$; here, we use $\varepsilon_1 = \varepsilon_2 = \varepsilon_3 = 10^{-2}$. In both cases, the starting point was the optimum design with respect to the minimum reflection level. The results are gathered in Table I (see also Fig. 2). For both antennas, the proposed relaxation approach results in a smaller footprint of the final design; for antenna II, the difference is dramatic (335 mm^2 versus 589 mm^2), which is due to the fact that this structure is much more complex than antenna I.

TABLE I
Antenna Optimization: Numerical Results

Problem formulation and optimization algorithm	Optimization results: size and $\max\lvert S_{11}\rvert$	
	Antenna I	Antenna II
Minimization of $\lvert S_{11}\rvert$	$A = 765$ mm^2 $S = -15.5$ dB	$A = 702$ mm^2 $S = -14.8$ dB
Size reduction [formulation (2), Sections II-A and II-B]	$A = 606$ mm^2 $S = -9.0$ dB	$A = 589$ mm^2 $S = -9.1$ dB
Size reduction (this work: objective relaxation, Section II-C)	$A = 583$ mm^2 $S = -9.9$ dB	$A = 335$ mm^2 $S = -9.6$ dB

At the same time, the proposed methodology allows for better satisfaction of the reflection requirement. It should be noted that this requirement cannot be satisfied exactly because the reflection constrained is not handled as a hard constraint; instead, it is controlled using a penalty function approach. The typical cost of the optimization process is between 10 and 20 iterations (3), which corresponds to 60–200 evaluations of the respective EM antenna model.

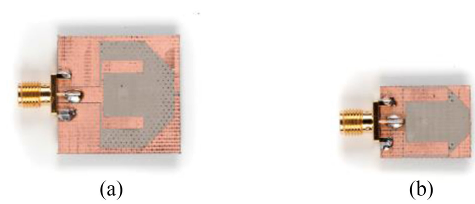

Fig. 3. Photographs of the fabricated antenna prototypes: (a) antenna II optimized for best matching, and (b) antenna II optimized for size using the proposed objective relaxation method.

C. Experimental Validation

For the sake of experimental validation, two designs of antenna II have been fabricated and measured in the anechoic chamber of Reykjavik University, Iceland. In order to achieve better agreement with simulation, the antenna has been redesigned with the SMA connector included in the computational model (the results of Section III-B were obtained without the connector). The first design (optimized for best matching) features 742 mm^2 footprint, whereas the area of the second design (optimized for size using the proposed relaxation method) is 329 mm^2. Fig. 3 shows the photographs of the antenna prototypes. Simulated and measured reflection characteristics have been shown in Fig. 4. Fig. 5 shows the simulated and measured H-plane radiation patterns for frequencies of 4, 6, 8, and 10 GHz. The agreement between simulation and measurements is acceptable. The primary reasons for misalignment are fabrication and assembly tolerances.

It can be observed that both antennas exhibit omnidirectional characteristics, particularly for frequencies 4 and 6 GHz. Reduction of the antenna size does not lead to any degradation

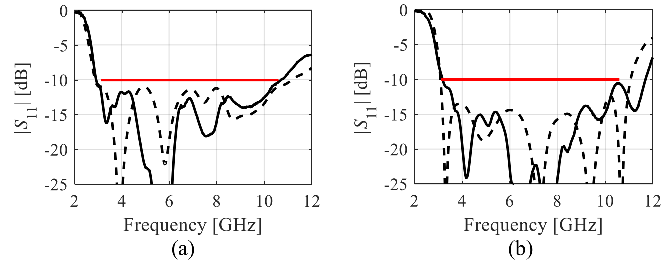

Fig. 4. Simulated (- - -) and measured (—) reflection characteristics for (a) antenna II optimized for best matching, and (b) antenna II optimized for size using the proposed objective relaxation method.

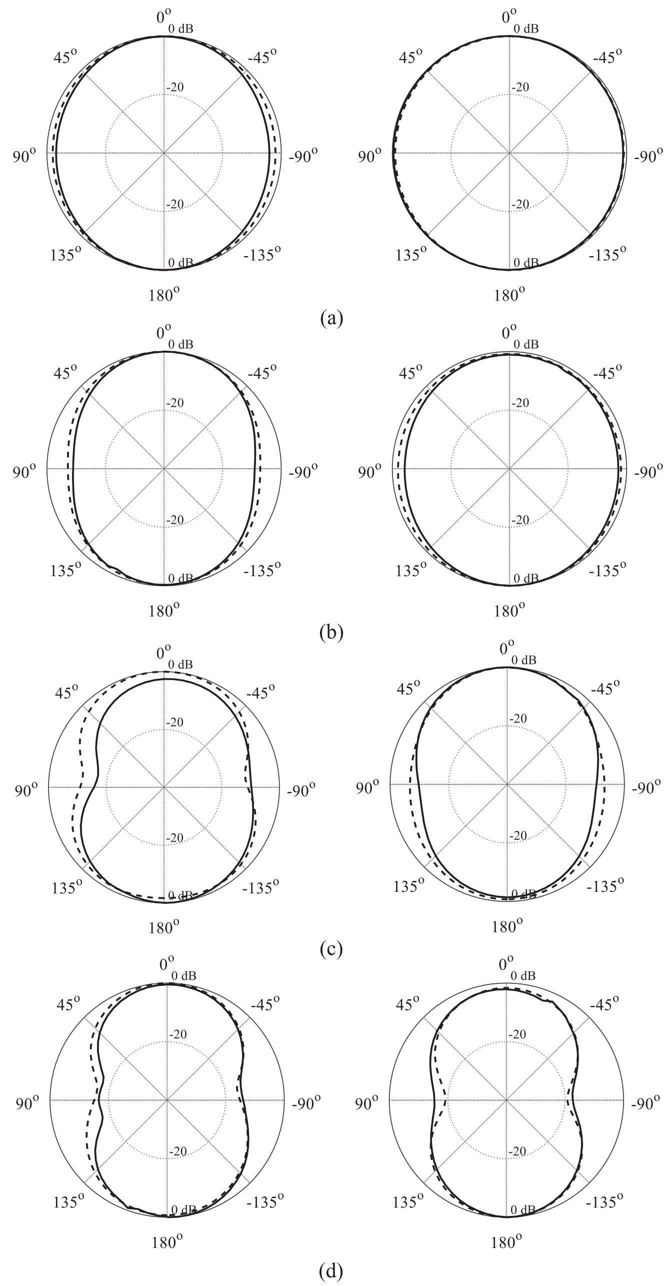

Fig. 5. Simulated (- - -) and measured (—) H-plane radiation patterns for antenna II optimized for best matching (left panel), and antenna II optimized for size using the proposed objective relaxation method (right panel): (a) 4 GHz, (b) 6 GHz, (c) 8 GHz, and (d) 10 GHz.

of the patterns. On the contrary, the miniaturized design exhibits even more regular characteristic than the structure optimized for best matching.

IV. Conclusion

A technique for reliable EM-driven size reduction of antenna structures has been proposed. Our approach exploits relaxation of design objectives, which allows for achieving smaller footprint area compared to conventional formulation of the design problem as demonstrated by examples. Numerical results have been validated experimentally. The future work will include more comprehensive validation of the technique as well as application for design cases with multiple constraints.

References

[1] X.-S. Yang, K.-T. Ng, S. H. Yeung, and K. F. Man, “Jumping genes multiobjective optimization scheme for planar monopole ultrawideband antenna,” *IEEE Trans. Antennas Propag.*, vol. 56, no. 12, pp. 3659–3666, Dec. 2008.

[2] M. Bod, H. R. Hassani, and M. M. S. Taheri, “Compact UWB printed slot antenna with extra Bluetooth, GSM, and GPS bands,” *IEEE Antennas Wireless Propag. Lett.*, vol. 11, pp. 531–534, 2012.

[3] H. Ning, *Unit and Ubiquitous Internet of Things*. Boca Raton, FL, USA: CRC Press, 2013.

[4] N. Chahat, M. Zhadobov, R. Sauleau, and K. Ito, “A compact UWB antenna for on-body applications,” *IEEE Trans. Antennas Propag.*, vol. 59, no. 4, pp. 1123–1131, Apr. 2011.

[5] L. Li, S. W. Cheung, and T. I. Yuk, “Compact MIMO antenna for portable devices in UWB applications,” *IEEE Trans. Antennas Propag.*, vol. 61, no. 8, pp. 4257–4264, Aug. 2013.

[6] A. Bekasiewicz and S. Koziel, “Compact UWB monopole antenna for Internet of things applications,” *Electron. Lett.*, vol. 52, no. 7, pp. 492–494, 2016.

[7] J.-F. Li, Q.-X. Chu, Z.-H. Li, and X.-X. Xia, “Compact dual band-notched UWB MIMO antenna with high isolation,” *IEEE Trans. Antennas Propag.*, vol. 61, no. 9, pp. 4759–4766, Sep. 2013.

[8] A. Bekasiewicz and S. Koziel, “A novel structure and design optimization of compact UWB slot antenna,” *Electron. Lett.*, vol. 52, no. 9, pp. 681–681, 2016.

[9] Y.-F. Liu, P. Wang, and H. Qin, “Compact ACS-fed UWB monopole antenna with extra Bluetooth band,” *Electron. Lett.*, vol. 50, no. 18, pp. 1263–1264, 2014.

[10] A. Bekasiewicz and S. Koziel, “Structure and computationally-efficient simulation-driven design of compact UWB monopole antenna,” *IEEE Antennas Wireless Propag. Lett.*, vol. 14, pp. 1282–1285, 2015.

[11] A. Bekasiewicz and S. Koziel, “A structure and EM-driven design of novel compact UWB slot antenna,” *Microw., Antennas Propag.*, vol. 11, no. 2, pp. 219–223, Jan. 2016.

[12] J. Nocedal and S. Wright, *Numerical Optimization*. New York, NY, USA: Springer, 2006.

[13] S. Koziel and L. Leifsson, *Simulation-Driven Design by Knowledge-Based Response Correction Techniques*. New York, NY, USA: Springer, 2016.

[14] K. Deb, *Multi-Objective Optimization Using Evolutionary Algorithms*. New York, NY, USA: Wiley, 2001.

[15] S. Koziel and S. Ogurtsov, *Antenna Design by Simulation-Driven Optimization. Surrogate-Based Approach*. New York, NY, USA: Springer, 2014.

[16] A. R. Conn, N. I. M. Gould, and P. L. Toint, *Trust Region Methods* (2000 MPS-SIAM Series on Optimization). Philadelphia, PA, USA: SIAM, 2000.

[17] B. Huang, Y. Yao, and Z. Feng, “Analysis and design of a novel compact UWB antenna,” in *Proc. Int. Conf. Microw. Millim. Wave Technol.*, vol. 4, 2008, pp. 1806–1809.

[18] X. Qing and Z. N. Chen, “Compact coplanar waveguide-fed ultra-wideband monopole-like slot antenna,” *Microw., Antennas Propag.*, vol. 3, no. 5, pp. 889–898, Aug. 2009.